JAIST Repository
https://dspace.jaist.ac.jp/

Title	Low-temperature-annealed Ohmic contacts to ultrathin-AlGaN/GaN heterostructures with no two-dimensional electron gas
Author(s)	Uryu, Kazuya; Deng, Yuchen; Nanjo, Takuma; Suzuki, Toshi-kazu
Citation	Applied Physics Letters, 126(23): 232103
Issue Date	2025-06-09
Type	Journal Article
Text version	publisher
URL	https://hdl.handle.net/10119/20614
Rights	Copyright (c) 2025 AIP Publishing. This article may be downloaded for personal use only. Any other use requires prior permission of the author and AIP Publishing. This article appeared in Kazuya Uryu, Yuchen Deng, Takuma Nanjo, Toshi-kazu Suzuki; Low-temperature-annealed Ohmic contacts to ultrathin-AlGaN/GaN heterostructures with no two-dimensional electron gas, Applied Physics Letters, 9 June 2025; 126 (23): 232103 and may be found at https://doi.org/10.1063/5.0260035.
Description	

JAIST
JAPAN
ADVANCED INSTITUTE OF
SCIENCE AND TECHNOLOGY

Japan Advanced Institute of Science and Technology

Applied Physics Letters ARTICLE pubs.aip.org/aip/apl

Low-temperature-annealed Ohmic contacts to ultrathin-AlGaN/GaN heterostructures with no two-dimensional electron gas

Cite as: Appl. Phys. Lett. **126**, 232103 (2025); doi: 10.1063/5.0260035
Submitted: 22 January 2025 · Accepted: 24 May 2025 ·
Published Online: 9 June 2025

View Online Export Citation CrossMark

Kazuya Uryu,[1,2,a] Yuchen Deng,[2] Takuma Nanjo,[3] and Toshi-kazu Suzuki[2]

AFFILIATIONS

[1]Advantest Laboratories Ltd., 48-2 Matsubara, Kami-Ayashi, Aoba-ku, Sendai, Miyagi 989-3124, Japan
[2]Center for Nano Materials and Technology, Japan Advanced Institute of Science and Technology (JAIST), 1-1 Asahidai, Nomi, Ishikawa 923-1292, Japan
[3]Mitsubishi Electric Corp., 8-1-1 Tsukaguchi-honmachi, Amagasaki, Hyogo 661-8661, Japan

[a]**Author to whom correspondence should be addressed:** kazuya.uryu@advantest.com

ABSTRACT

We investigated low-temperature-annealed Ohmic contacts to ultrathin-AlGaN/GaN heterostructures with no two-dimensional electron gas (2DEG), which have extremely high sheet resistances of $\sim 10^{12}\,\Omega/\square$. The Ohmic contacts are formed by metal deposition and low-temperature annealing at $< 600\,^{\circ}\mathrm{C}$, where a contact resistance down to $\simeq 0.74\,\Omega\,\mathrm{mm}$ can be realized. In order to evaluate the sheet resistance ρ_s, the sheet electron concentration n_s, and the electron mobility μ_s of the AlGaN/GaN under the Ohmic-metals, we fabricated and characterized multi-probe Hall devices. As a result, we find ρ_s significantly decreased down to $\sim 600\,\Omega/\square$, n_s in the $10^{12}\,\mathrm{cm}^{-2}$ range, and $\mu_s > 1000\,\mathrm{cm}^2/\mathrm{V\text{-}s}$ under the Ohmic-metals, where the relationship between n_s and μ_s suggests that a 2DEG is formed at the AlGaN/GaN heterointerface. The specific contact resistivity weakly depends on both n_s and the measurement temperature, being well explained by direct tunneling between the formed 2DEG and the Ohmic-metal. Furthermore, it is found that the sheet resistance after Ohmic-metal removal returns to the initial value of $\sim 10^{12}\,\Omega/\square$. One possible hypothesis to explain this is that polarization doping takes place under the Ohmic-metals.

Published under an exclusive license by AIP Publishing. https://doi.org/10.1063/5.0260035

13 June 2025 04:46:58

In order to realize GaN-based normally-off field-effect transistors (FETs), gate-recess methods using dry etching have been widely employed.[1–4] However, there are several issues with these methods, such as crystal damage, which leads to a degradation in the electron transport properties,[4] and difficulty in controlling the etching depth. On the other hand, using ultrathin-AlGaN/GaN heterostructures with no two-dimensional electron gas (2DEG), normally-off FETs without dry etching have been reported,[5–10] where the 2DEG is selectively induced in the access region owing to an insulator deposition.[7,11] Ohmic contacts to the ultrathin-AlGaN/GaN heterostructures have been formed by a metal deposition and high-temperature annealing at $> 800\,^{\circ}\mathrm{C}$ without ion implantations, giving the contact resistance R_c of 1.3 or 3.4 $\Omega\,\mathrm{mm}$.[7,10] However, since high-temperature annealing wastes the thermal budget and leads to rough surface morphology and poor edge acuity[12] of the Ohmic-metals, low-temperature annealing at $< 600\,^{\circ}\mathrm{C}$ is desired in practice. While low-temperature-annealed Ohmic contacts with low contact resistances $R_c < 1\,\Omega\,\mathrm{mm}$ are obtained for thick-AlGaN/GaN heterostructures with 2DEG,[12–17] the possibility of low-temperature-annealed Ohmic contacts for ultrathin-AlGaN/GaN heterostructures with no 2DEG has been unclear.

In this work, we investigated low-temperature-annealed ($< 600\,^{\circ}\mathrm{C}$) Ohmic contacts for ultrathin-AlGaN/GaN heterostructures with no 2DEG having extremely high sheet resistances, where it was found that low contact resistances $R_c < 1\,\Omega\,\mathrm{mm}$ can be realized despite the depletion of 2DEG and extremely high sheet resistances of the heterostructures. Moreover, by using multi-probe Hall measurements,[18–20] we evaluated the sheet resistance ρ_s, the carrier concentration n_s, and the carrier mobility μ_s under the low-temperature-annealed Ohmic-metals. In general, Ohmic-metal formation modifies properties inside the semiconductor under the formed Ohmic-metal;[21,22] ρ_s, n_s, and μ_s under the Ohmic-metal differ from those before the Ohmic-metal formation and can be characterized by multi-probe Hall measurements. We find significantly decreased ρ_s, increased n_s, and high μ_s under the low-temperature-annealed Ohmic-metal, where the relationship between n_s and μ_s suggests that a 2DEG is formed at the AlGaN/GaN heterointerface. From the

Published under an exclusive license by AIP Publishing

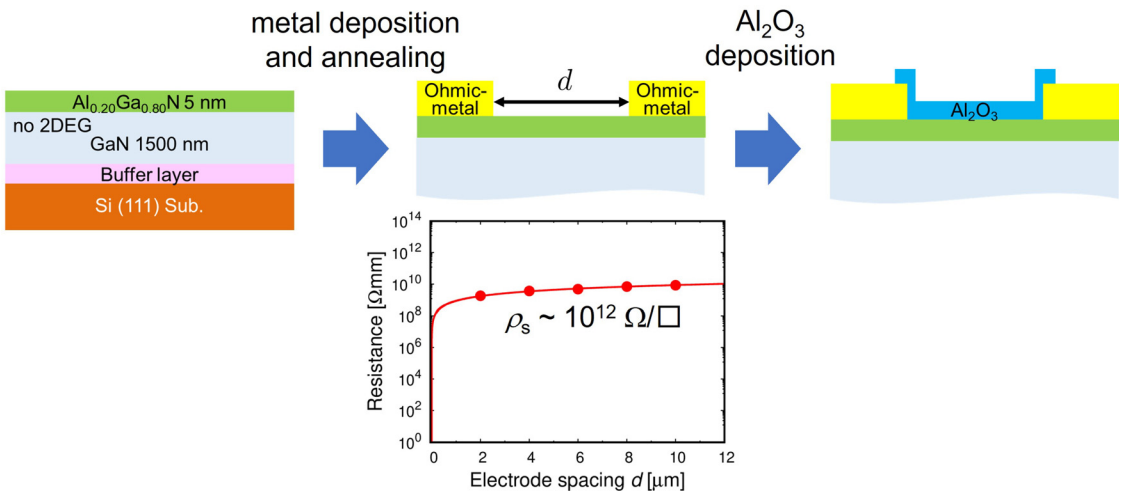


FIG. 1. The fabrication process of transfer length method (TLM) samples using the ultrathin-AlGaN/GaN heterostructures. Bottom: the TLM measurement results after metal deposition and annealing.

dependence of the specific contact resistivity ρ_c on n_s and measurement temperature, we discuss a conduction mechanism between the 2DEG and the Ohmic-metal. In addition, it is shown that the sheet resistance after Ohmic-metal removal returns to the initial extremely high value, suggesting a mechanism of the 2DEG formation under the Ohmic-metal.

According to the process flow shown in Fig. 1, we fabricated transfer length method (TLM) samples using an $Al_{0.20}Ga_{0.80}N$ (5 nm)/GaN (1500 nm) heterostructure grown by metal-organic chemical vapor deposition on Si (111). The thickness of the AlGaN layer is so thin that the 2DEG is fully depleted. The Ohmic-metal was formed by Ta/Al/Ta metal deposition and subsequent annealing at 575 °C in N_2 ambient. At this stage, from the TLM measurement results shown in the bottom of Fig. 1 with linear fitting, we can confirm an extremely high sheet resistance $\sim 10^{12}$ Ω/□ between the Ohmic-metals. On the other hand, the contact resistance R_c cannot be accurately evaluated due to the extremely high sheet resistance; the vertical intercept for the linear fitting is quite uncertain. In order to give conductivity between the Ohmic-metals, an Al_2O_3 insulator with a thickness of ~ 100 nm was deposited by atomic layer deposition using trimethylaluminum and oxygen plasma at 300 °C. Then, we carried out TLM measurements, whose results are shown in Fig. 2, from which R_c can be accurately evaluated. We obtain a low $R_c \simeq 0.74$ Ω mm, as well as a significantly reduced sheet resistance $\simeq 1080$ Ω/□ under the Al_2O_3 insulator owing to band bending.[7] This indicates that $R_c < 1$ Ω mm can be realized by low-temperature annealing despite the depletion of 2DEG and the extremely high sheet resistance of the heterostructure. If we employ annealing at further decreased temperatures 525 and 475 °C, R_c and its sample-to-sample deviation are increased as shown in the inset of Fig. 2.

In order to characterize the semiconductor properties under the Ohmic-metals, we fabricated multi-probe Hall devices[18–20] shown in Fig. 3, where the Ohmic-metals with a length $L = 200$ μm and a width $W = 2, 5, 10, 20$ μm are formed by annealing at 575 °C. The devices have measurement electrodes consisting of current injection and multiple voltage probe electrodes. In the access regions between the Ohmic-metal and the measurement electrodes, the Al_2O_3 insulator is deposited. Using the multi-probe Hall devices, we can obtain the distribution of the lateral and Hall voltages inside the semiconductor separately from the Ohmic-metal. As defined in Fig. 3, applying a current density J_0 (mA/mm) through the current injection electrodes, we measured the lateral voltage V_L under no magnetic field $B = 0$ and the Hall voltage V_H under $B = 0.32$ T, as a function of the position x using the voltage probe electrodes. Figure 4 (left) shows the measured V_L/J_0 as a function of the position x. We observe a nonlinear behavior independent of W, which can be analyzed based on a transmission line model[18] giving

$$\frac{V_L(x)}{J_0} = -\frac{\rho_s}{\rho_s + \rho_m}\left(\rho_m x + \rho_s \frac{\sinh(x/L_T)}{L_T \cosh(L/2L_T)}\right), \quad (1)$$

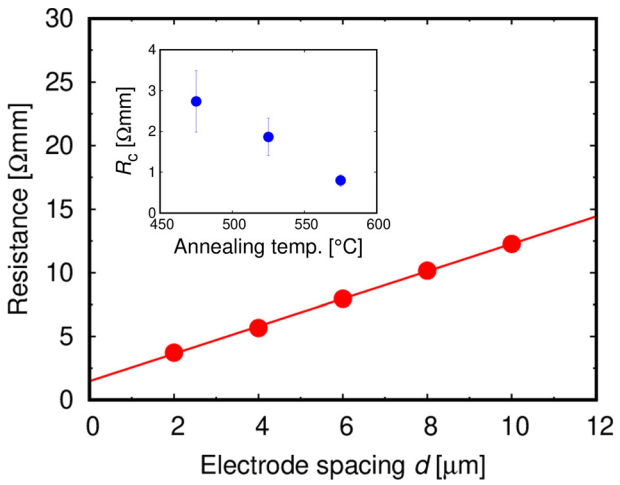


FIG. 2. The TLM measurement result for the Ohmic contacts annealed at 575 °C. The inset: the contact resistance R_c as a function of annealing temperature.

13 June 2025 04:46:58

Published under an exclusive license by AIP Publishing

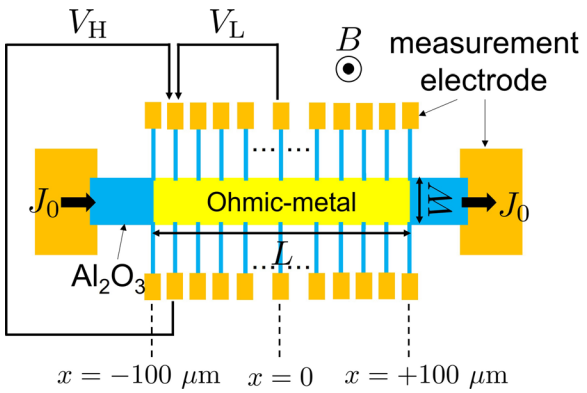


FIG. 3. The schematic structure of the multi-probe Hall devices, where the Al_2O_3 insulator is deposited on the access regions between the Ohmic-metal and the measurement electrodes.

where ρ_m is the Ohmic-metal sheet resistance, $L_T = \sqrt{\rho_c/(\rho_s + \rho_m)}$ is the characteristic length, and ρ_c is the specific contact resistivity. The measured results are well fitted using (1), giving $\rho_s \simeq 600\ \Omega/\square$ under the Ohmic-metal, $\rho_m \simeq 0.20\ \Omega/\square$, $\rho_c \simeq 0.95 \times 10^{-5}\ \Omega\,cm^2$, and $R_c \simeq \sqrt{\rho_s \rho_c} = 0.74\ \Omega\,mm$. We find that, under the Ohmic-metal, ρ_s is significantly decreased from the extremely high initial value $\sim 10^{12}\ \Omega/\square$. Figure 4 (center) shows the measured V_H/J_0W as a function of the position x. We obtain the measured mobility $\mu_{meas} = V_H/(BW\partial V_L/\partial x)|_{x=0}$ dependent on W, which can be fitted by[20]

$$\mu_{meas} \simeq \mu_s - \frac{\rho_s(\mu_s - \mu_m)}{\rho_s + \rho_m}\left(1 - \frac{\tanh(W/2L_T)}{W/2L_T}\right) \quad (2)$$

using the electron mobility μ_m in the Ohmic-metal as shown in Fig. 4 (right). The fitting gives $\mu_s \simeq 1250\ cm^2/V\text{-}s$, $\mu_m \sim 20\ cm^2/V\text{-}s$, and consequently $n_s = 1/q\rho_s\mu_s \simeq 8.3 \times 10^{12}\ cm^{-2}$ under the Ohmic-metal; we find significant increase in n_s and high μ_s.

The same characterization was carried out for the Ohmic contact annealed at 525 and 475 °C, summarized in Table I. The annealing decreases ρ_s, ρ_c, and R_c, associated with an increase in n_s with high μ_s. Figure 5 plots the relationship between the measured n_s and μ_s under the Ohmic-metals, where that under Al_2O_3 obtained by conventional Hall measurements is simultaneously plotted. The relationship can be fitted by the theoretical curve for 2DEG given in Fig. 5, where we consider polar optical phonon (PO),[23] acoustic phonon (AC),[24,25] barrier alloy (BA),[24] interface charge (IC),[24] and interface roughness[26–28] scatterings. The obtained electron mobilities $\mu_s > 1000\ cm^2/V\text{-}s$ are quite higher than a possible electron mobility in the AlGaN layer of $\sim 300\ cm^2/V\text{-}s$ (Ref. 29) as well as that in the Ohmic-metal of $\mu_m \sim 20\ cm^2/V\text{-}s$. This indicates that the measured μ_s and n_s are dominated by 2DEG generation at the AlGaN/GaN heterointerface. Furthermore, it is suggested that ionized impurity scattering associated with donors, such as nitrogen vacancies,[12,30] does not take place.

Figure 6 shows the relationship between ρ_c and n_s, where we find decrease in ρ_c with an increase in n_s, but the dependence is not so strong. This dependence can be explained by direct tunneling between the 2DEG and the Ohmic-metals shown in the inset of Fig. 6. The direct tunnel current is given by

$$J = \int_{E_0}^{\infty} \frac{eD_2}{\tau}[f(E - E_F - eV) - f(E - E_F)]dE, \quad (3)$$

where τ is the tunneling escape time, $D_2 = m^*/\pi\hbar^2$ is the 2D density of states, $f(E-\mu) = [1 + \exp((E-\mu)/k_BT)]^{-1}$ is the Fermi distribution function, E_F is the Fermi energy, and E_0 is the 2DEG ground state energy. Thus, the direct tunnel conductance is

$$G = 1/\rho_c = \left.\frac{\partial J}{\partial V}\right|_{V=0} = \frac{e^2D_2}{\tau}\int_{E_0}^{\infty}[-f'(E - E_F)]\,dE$$
$$= \frac{e^2D_2}{\tau}\left(1 - \exp\left(-\frac{n_s}{D_2k_BT}\right)\right), \quad (4)$$

where we use $n_s \simeq D_2k_BT\ln(1 + e^{(E_F - E_0)/k_BT})$, assuming that all the electrons of the 2DEG lie in the ground state. The measurement result is well fitted by (4), leading to $\tau \simeq 160$ ps.

From (4), it is expected that ρ_c is slightly increased with an increase in temperature. In order to confirm this, we measured ρ_c at 300–370 K for the Ohmic contact annealed at 575 °C. Figure 7(a) shows the measurement temperature dependence of ρ_c, which is obtained by measurements of $V_L(x)$ shown in the inset. The temperature dependence of ρ_c obeys the theoretical curve given by (4) with $n_s \simeq 8.3 \times 10^{12}\ cm^{-2}$ and $\tau \simeq 160$ ps. As expected, we observe the slight increase in ρ_c with temperature; this is quite in contrast to that for Ohmic contacts to thick-AlGaN/GaN heterostructures and n-GaN dominated by the thermionic field or field emission.[18–20]

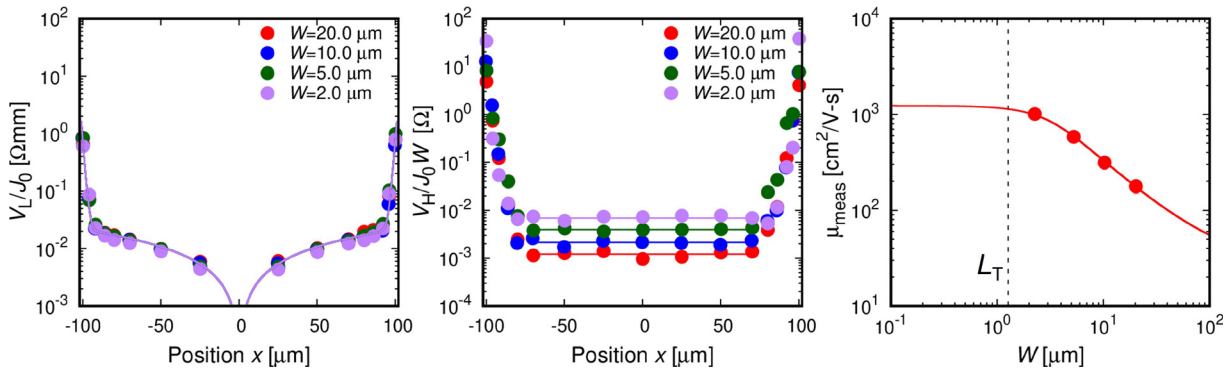


FIG. 4. The measured $V_L(x)/J_0$ (left), $V_H(x)/J_0W$ (center), and μ_{meas} as a function of W (right) with the fitting curves for the Ohmic-metal annealed at 575 °C.

13 June 2025 04:46:58

Published under an exclusive license by AIP Publishing

TABLE I. Summary of the multi-probe Hall measurements.

	ρ_s ($\Omega/\square$)	ρ_c ($10^{-5}\,\Omega\,cm^2$)	R_c (Ω mm)	L_T (μm)	μ_s (cm^2/V-s)	n_s ($10^{12}\,cm^{-2}$)
Annealed at 575 °C	600	0.95	0.74	1.2	1250	8.3
Annealed at 525 °C	1800	2.0	1.9	1.1	1560	2.2
Annealed at 475 °C	3200	2.3	2.7	0.85	1340	1.5

Moreover, from the measurements of $V_L(x)$, we obtain the temperature dependence of ρ_s as shown in Fig. 7(b). Assuming the temperature independent $n_s \simeq 8.3 \times 10^{12}\,cm^{-2}$, the results indicate the electron mobility decreasing from 1250 cm^2/V-s at 300 K to 850 cm^2/V-s at 370 K. As shown by the fitting curve in Fig. 7(b), this can be well explained by the temperature dependent 2DEG mobility governed by the scattering mechanisms as in Fig. 5, polar optical phonon (PO), acoustic phonon (AC), barrier alloy (BA), interface charge (IC), and interface roughness (IR) scatterings. These strongly support our picture based on the 2DEG formation at the heterointerface and the direct tunnel conduction between the induced 2DEG and the Ohmic-metal.

Moreover, we examined removal of the low-temperature-annealed Ohmic-metal. As depicted in Fig. 8, we fabricated circular TLM samples for the heterostructures before Ohmic-metal formation (initial) and after Ohmic-metal removal, with TLM electrodes of a radius $a = 40\,\mu$m and a gap length $b = 4$–$10\,\mu$m. For the former sample, Ohmic-metals for the TLM electrodes have been formed by annealing at 575 °C. For the latter sample, first a large Ohmic-metal

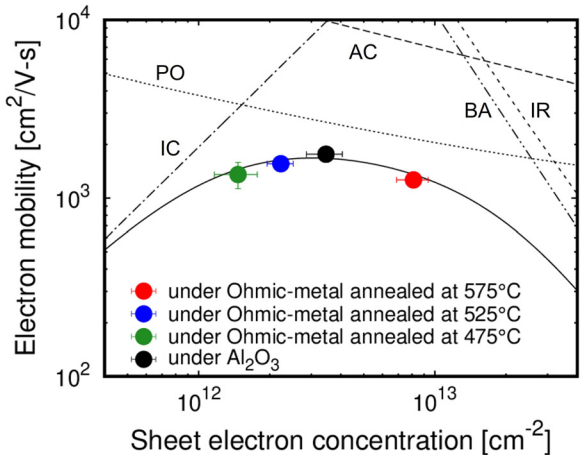


FIG. 5. The relationship between n_s and μ_s under the Ohmic-metals and the Al_2O_3 insulator with the theoretical curve for 2DEG.

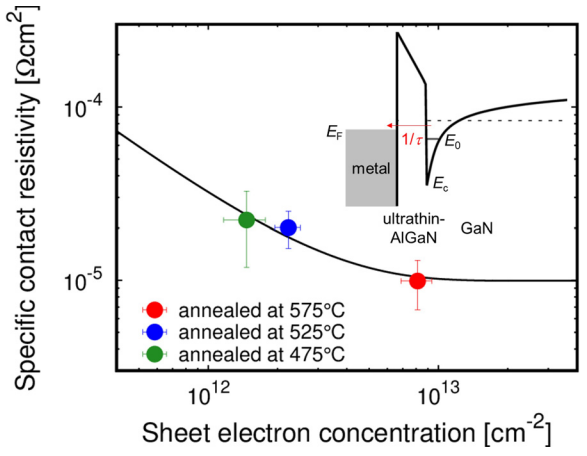


FIG. 6. The relationship between n_s and ρ_c. The inset: Direct tunneling between the 2DEG and the Ohmic-metal.

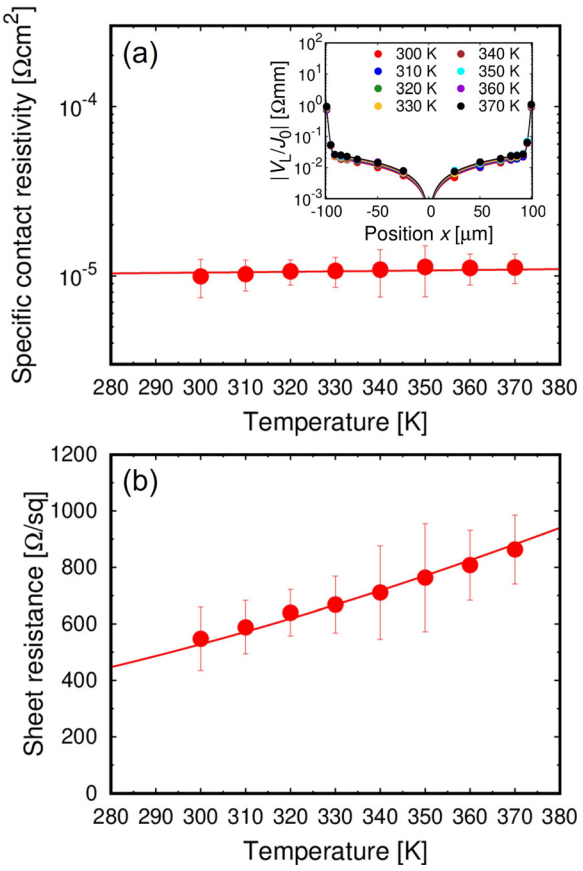


FIG. 7. The temperature dependence of (a) the specific contact resistivity ρ_c and (b) the sheet resistance ρ_s for the Ohmic contacts annealed at 575 °C with the fitting curves. The inset of (a): $V_L(x)/J_0$ measured at 300–370 K.

13 June 2025 04:46:58

Published under an exclusive license by AIP Publishing

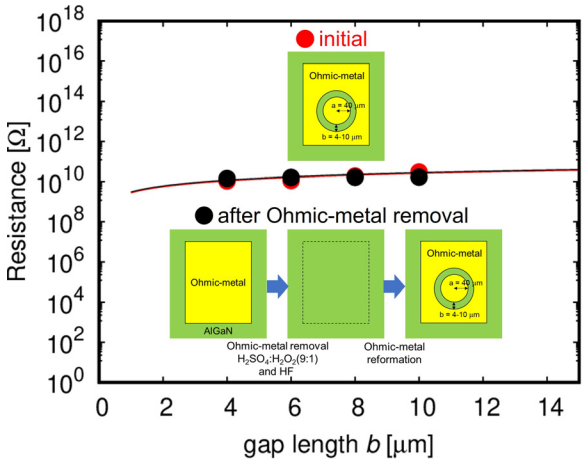


FIG. 8. The circular TLM measurement results for the heterostructures before Ohmic-metal formation (initial) and after Ohmic-metal removal.

was formed by annealing at 575 °C, next, the Ohmic-metal was wet-etched by H_2SO_4:H_2O (9:1) and HF, and subsequently, Ohmic-metals for the TLM electrodes have been formed by annealing at 575 °C. The measurement results in Fig. 8 show sheet resistances of $\sim 10^{12}\,\Omega/\square$ for both circular TLM samples, indicating that the decreased ρ_s under the Ohmic-metal returns to the initial extremely high value. Thus, we conclude that donors, such as nitrogen vacancies, are not formed under the Ohmic-metal. On the other hand, in order to explain the increase in n_s under the Ohmic-metal up to $\simeq 8.3 \times 10^{12}\,\mathrm{cm}^{-2}$ only by a metal barrier height (without doping), it is necessary to assume a barrier height $\lesssim 0.1$ eV, which is too small for Ta-based Ohmic-metals.[17,19] Thus, "doping without donors" under the Ohmic-metal is suggested. As a possible hypothesis, we consider that polarization doping takes place by strain, similar to the cases for thick-AlGaN/GaN heterostructures and n-GaN.[18–20]

In summary, we investigated low-temperature-annealed Ohmic contacts to ultrathin-AlGaN/GaN heterostructures with no 2DEG, which have extremely high sheet resistances. The Ta/Al/Ta Ohmic-metal with the contact resistance of $R_c \simeq 0.74\,\Omega$mm can be realized by annealing at 575 °C. The multi-probe Hall measurements elucidated that a 2DEG is formed at the AlGaN/GaN heterointerface under the Ohmic-metal. We conclude that direct tunneling between the formed 2DEG and the Ohmic-metal dominates the contact resistance. Furthermore, it is shown that the sheet resistance after Ohmic-metal removal returns to the initial extremely high value, indicating that donors, such as nitrogen vacancies, are not formed under the Ohmic-metals. We consider that doping under the Ohmic-metals without donors takes place. Polarization doping is a possible hypothesis to explain the results.

This work was supported by JSPS KAKENHI Grant Nos. JP22H01545 and JP23K22815.

AUTHOR DECLARATIONS

Conflict of Interest

The authors have no conflicts to disclose.

Author Contributions

Kazuya Uryu: Data curation (lead); Formal analysis (equal); Investigation (lead); Methodology (equal); Writing – original draft (lead). **Yuchen Deng:** Investigation (supporting); Writing – review & editing (supporting). **Takuma Nanjo:** Resources (lead). **Toshi-kazu Suzuki:** Conceptualization (lead); Formal analysis (equal); Funding acquisition (lead); Methodology (equal); Project administration (lead); Supervision (lead); Writing – review & editing (lead).

DATA AVAILABILITY

The data that support the findings of this study are available from the corresponding author upon reasonable request.

REFERENCES

[1]V. Kumar, A. Kuliev, T. Tanaka, Y. Otoki, and I. Adesida, Electron. Lett. **39**, 1758 (2003).
[2]T. Oka and T. Nozawa, IEEE Electron Device Lett. **29**, 668 (2008).
[3]T. Sato, K. Uryu, J. Okayasu, M. Kimishima, and T. Suzuki, Appl. Phys. Lett. **113**, 063505 (2018).
[4]D. D. Nguyen, T. Isoda, Y. Deng, and T. Suzuki, J. Appl. Phys. **130**, 014503 (2021).
[5]H. Otake, S. Egami, H. Ohta, Y. Nanishi, and H. Takasu, Jpn. J. Appl. Phys., Part 2 **46**, L599 (2007).
[6]J. Derluyn, M. Van Hove, D. Visalli, A. Lorenz, D. Marcon, P. Srivastava, K. Geens, B. Sijmus, J. Viaene, X. Kang, J. Das, F. Medjdoub, K. Cheng, S. Degroote, M. Leys, G. Borghs, and M. Germain, in *IEEE International Electron Devices Meeting (IEDM)* (IEEE, 2009).
[7]S. Huang, X. Liu, X. Wang, X. Kang, J. Zhang, Q. Bao, K. Wei, Y. Zheng, C. Zhao, H. Gao, Q. Sun, Z. Zhang, and K. J. Chen, IEEE Electron Device Lett. **37**, 1617 (2016).
[8]S. Huang, X. Liu, X. Wang, X. Kang, J. Zhang, J. Fan, J. Shi, K. Wei, Y. Zheng, H. Gao, Q. Sun, M. Wang, B. Shen, and K. J. Chen, IEEE Trans. Electron Devices **65**, 207 (2018).
[9]H. Jiang, R. Zhu, Q. Lyu, C. W. Tang, and K. M. Lau, Semicond. Sci. Technol. **36**, 034001 (2021).
[10]T. Nanjo, T. Imazawa, A. Kiyoi, T. Hayashida, T. Watahiki, and N. Miura, Jpn. J. Appl. Phys., Part 1 **61**, SC1015 (2022).
[11]T. Nanjo, H. Koyama, T. Imazawa, A. Kiyoi, A. Imai, T. Hayashida, T. Watahiki, Y. Yamamoto, and N. Miura, Electron. Lett. **57**, 670 (2021).
[12]A. Malmros, H. Blanck, and N. Rorsman, Semicond. Sci. Technol. **26**, 075006 (2011).
[13]M. Van Hove, S. Boulay, S. R. Bahl, S. Stoffels, X. Kang, D. Wellekens, K. Geens, A. Delabie, and S. Decoutere, IEEE Electron Device Lett. **33**, 667 (2012).
[14]A. Pooth, J. Bergsten, N. Rorsman, H. Hirshy, R. Perks, P. Tasker, T. Martin, R. Webster, D. Cherns, M. Uren, and M. Kuball, Microelectron. Reliab. **68**, 2–4 (2017).
[15]J. Zhang, X. Kang, X. Wang, S. Huang, C. Chen, K. Wei, Y. Zheng, Q. Zhou, W. Chen, B. Zhang, and X. Liu, IEEE Electron Device Lett. **39**, 847 (2018).
[16]Y.-K. Lin, J. Bergsten, H. Leong, A. Malmros, J.-T. Chen, D.-Y. Chen, O. Kordina, H. Zirath, E. Y. Chang, and N. Rorsman, Semicond. Sci. Technol. **33**, 095019 (2018).
[17]A. Calzolaro, R. Hentschel, I. F. Edokam, V. Sizov, T. Mikolajick, and A. Wachowiak, Semicond. Sci. Technol. **35**, 075011 (2020).
[18]K. Uryu, S. Kiuchi, and T. Suzuki, Appl. Phys. Lett. **119**, 023505 (2021).
[19]K. Uryu, S. Kiuchi, T. Sato, and T. Suzuki, Appl. Phys. Lett. **120**, 052104 (2022).
[20]K. Uryu, Y. Deng, S. P. Le, and T. Suzuki, AIP Adv. **13**, 075002 (2023).
[21]D. K. Schroder, *Semiconductor Material and Device Characterization* (John Wiley & Sons, Ltd., 2005), p. 147.
[22]H. Morkoç, *Handbook of Nitride Semiconductors and Devices, Electronic and Optical Processes in Nitrides* (John Wiley & Sons, Ltd, 2008), p. 41.
[23]C. Luan, Z. Lin, Y. Lv, J. Zhao, Y. Wang, H. Chen, and Z. Wang, J. Appl. Phys. **116**, 044507 (2014).

13 June 2025 04:46:58

Published under an exclusive license by AIP Publishing

[24]L. Hsu and W. Walukiewicz, Phys. Rev. B **56**, 1520 (1997).
[25]E. A. Henriksen, S. Syed, Y. Ahmadian, M. J. Manfra, K. W. Baldwin, A. M. Sergent, R. J. Molnar, and H. L. Stormer, Appl. Phys. Lett. **86**, 252108 (2005).
[26]A. Gold, Phys. Rev. B **35**, 723 (1987).
[27]H. Sakaki, T. Noda, K. Hirakawa, M. Tanaka, and T. Matsusue, Appl. Phys. Lett. **51**, 1934 (1987).
[28]O. Katz, A. Horn, G. Bahir, and J. Salzman, IEEE Trans. Electron Devices **50**, 2002 (2003).
[29]S. Bajaj, T.-H. Hung, F. Akyol, D. Nath, and S. Rajan, Appl. Phys. Lett. **105**, 263503 (2014).
[30]S. Ruvimov, Z. Liliental-Weber, J. Washburn, D. Qiao, S. S. Lau, and P. K. Chu, Appl. Phys. Lett. **73**, 2582 (1998).

13 June 2025 04:46:58

Published under an exclusive license by AIP Publishing